Simulation of acoustic radiation of an AC servo drive

David Franck, Michael van der Giet and Kay Hameyer
Institute of Electrical Machines, RWTH Aachen University, Aachen, Germany

Abstract

Purpose – Nowadays, the determination of the acoustic radiation of electric machines is of particular interest, because legal regulations restrict the maximum audible noise radiated by technical devices such as electrical machinery. The purpose of this paper is to analyze the electromagnetic excited structure-borne sound and air-borne noise of an AC servo drive.

Design/methodology/approach – This paper presents the required steps for the multiphysics acoustic simulation of electrical machines to evaluate its noise behaviour. This numerical approach starts with the electromagnetic force-wave simulation. The computation by a structure dynamic model determines the deformation of the mechanical structure due to the force-waves. The final step of the simulation approach consists of the computation of the acoustic radiation.

Findings – For the electromagnetic simulation analytical and numerical methods are combined to gain some acceleration of the entire multiphysics simulation approach. This combination offers additionally a detailed understanding of the noise generation mechanism in electrical machines.

Originality/value – Particular attention is paid to the structural-dynamic model. Modelling of microstructures, such as the laminated iron core or insulated coils, is memory and computational expensive. A systematic material homogenisation technique, based on experimental- and numerical modal analyses, yields a higher accuracy at lower computational costs when compared to standard numerical approaches. The presented multiphysics simulation is validated by measurements. The methods are presented by means of a case study.

Keywords Electromagnetism, Acoustic properties, Amplifiers, Radiation

Paper type Research paper

Introduction

Owing to the customers' demands and legal regulations, the acoustic radiation is attracting more importance during the development process of electrical machines. Accurate and automated simulation models are required for the detailed study of the exact causes of the radiated acoustic noise. In this paper, a multiphysics simulation approach, applying weak numerical coupling of the underlying models, is applied. A case study for an example permanent magnet synchronous motor is presented. In this regards, a coupling of electromagnetic simulation to determine the exciting forces, which act on the stator of the machine, a structural-dynamic simulation to calculate the displacement of the stator surface and an acoustic simulation to estimate the radiated sound pressure is established. A flow chart of the mentioned simulation chain is shown in Figure 1. In contrast to classical approaches the mechanical material parameters of laminated stator iron core is homogenised for the structural-dynamic model. By experimental and numeric modal analysis the mechanical material parameters, Young's modulus, Poisson ratio and shear modulus, are determined by applying an optimisation algorithm. This results in a significant improvement in the model accuracy and reduces the computational costs of the structural-dynamic simulation. The aim of the multiphysics model presented is the prediction of the acoustic behaviour of the studied servo drive.

COMPEL: The International Journal for Computation and Mathematics in Electrical and Electronic Engineering
Vol. 29 No. 4, 2010
pp. 1060-1069

0332-1649
DOI 10.1108/03321641011044479

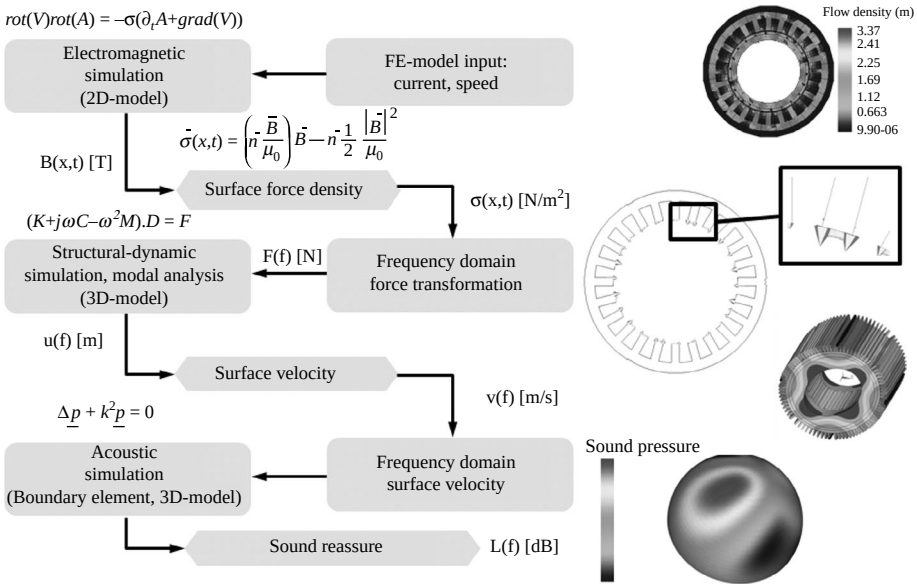

Figure 1.
Flow chart representing the multiphysics simulation approach

Electromagnetic simulation

The essential part of the multiphysics simulation approach is the electromagnetic computation since the electromagnetic field generates force-waves exciting the stator lamination and housing of the motor. Owing to the homogenous structure in axial direction of the studied motor, a two dimensional magnetic finite element (FE) model is used. The flux density distribution is calculated for one rotation of the rotor with a mechanical rotation angle of one degree per step. The next computational steps are distinguished into analyses of noise sources and the computation of the electromagnetically excited force-waves.

To study the sources of the electromagnetically excited noise in a first step only the normal component of the flux density waves is considered. This simplification is valid, because the magnitude of the normal components is dominant when compared to the tangential component and the aim of this analysis step is not to exact determine force-wave amplitudes and phase angles, but to identify the cause of particular electromagnetical force excitations. The resulting air gap field is studied in frequency and pole domain. Therefore, the air gap flux density is modal decomposed by a 2D-DFT in space and time. It, hence, can be described by a Fourier-series with the magnitude $B_{i,j}$ of each flux density wave, the ordinal number ν_j, the frequency f_i and the phase angle $\varphi_{i,j}$ by:

$$B(x,t) = \sum_{i=-i_{\max}}^{i_{\max}} \sum_{j=1}^{j_{\max}} B_{i,j} \cdot \cos(2\pi f_i \cdot t - \nu_j \cdot x - \varphi_{i,j}). \quad (1)$$

whereby i represents the frequency order, i_{max} is determined by the number of calculated simulation steps per period, j represents the circumferential order and j_{max} is given by the

number of flux density samples in the air gap. In contrast to classical approaches, in which the force density is Fourier-decomposed after calculating it from multiplication of the flux density in time domain, here the force density waves σ are determined by applying a convolution of the flux density waves with themselves (equation (1)) (van der Giet *et al.*, 2009). In this case, the simplified Maxwell stress tensor is applied, not considering the tangential flux density components. A representation of the numerically sampled force density waves as a Fourier-series can be given by:

$$\sigma(x,t) = \sum_{k=1}^{k_{\max}} \sum_{l=1}^{l_{\max}} \hat{\sigma}_{k,l} \cdot \cos(2\pi(f_k \pm f_l) \cdot t - (\nu_k \pm \nu_l) \cdot x - (\varphi_k \pm \varphi_l)). \tag{2}$$

With this approach, a decomposition of the force-density waves into trigonometric combinations of flux density waves is possible. In connection with classical analytical approaches (Jordan, 1950; Gieras *et al.*, 2006; Herranz Gracia, 2008) the components of this force density wave can be mapped to the known causes, which can be the spatial or parametric harmonics, such as slotting and winding space harmonics, harmonics caused by the teeth saturation, eccentricity fields, etc. The advantage of this approach is the in-depth insight into the generation and cause of the force density waves (van der Giet *et al.*, 2009). This Fourier-decomposed force density waves are studied individually for each frequency and ordinal number. In the following the resultant force density wave with the frequency equal to two times the pole-pair number p and the circumferential mode $\nu = 2$ presented as an example. This force density wave σ_{tot} and its decomposition in the three most important components σ_A, σ_B and σ_C is depicted in a space vector diagram (Figure 2). It has to be noted that all less important, respectively, smaller components, which are not drawn in Figure 2, will close the gap between the tip of vector σ_{tot} and σ_C. The dominant component σ_A can be identified as superposition of the combination of the flux density waves of stator winding- and rotor space harmonics, as well as the stator space harmonics and the reluctance field. The frequencies and ordinal numbers of the flux density waves, which are involved in the generation of σ_A, σ_B and σ_C are collected in Table I. The decomposition of these three force waves into flux-density waves is shown in Table II. The flux density waves are mapped to the before mentioned sources and are defined by frequency and pole-pair number. The result of this analysis step is the determination of the most significant noise sources and their interpretation respective cause. These results are used for the acoustic optimisation of the studied motor. In particular, the winding scheme,

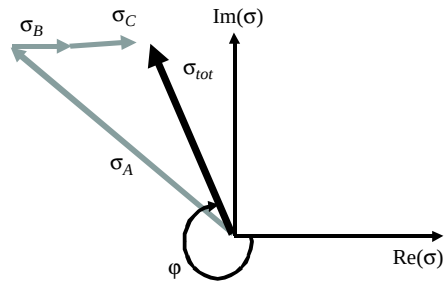

Figure 2.
Space vector representation of the force wave $f = 2pf_0$ and $\nu = 2$

rotor pole-pair number and the stator's slot number are sensitive parameters concerning the noise excitation of this motor.

In the next step, the surface-force density is calculated from the flux density distribution by using the Maxwell-stress tensor in time domain. In contrast to the previous analysis step of the electromagnetic noise causes, both, the normal and tangential components of the flux density are considered. For the multiphysics simulation chain the influence of the tangential flux density component is significant, particularly the phase angle of the force density waves is important. The flux density is evaluated on the interface between the air gap and the iron stator teeth. In this way the non-linear characteristics of the iron can be taken into account.

Material parameter optimisation

The deformation of the stator can be calculated from the calculated force densities acting on the stator teeth. The vibrational behaviour of the stator system is strongly dependent on its material properties (Garvey, 1989). Therefore, a detailed knowledge of all associated material parameters is required. In general, mechanical material parameters for structures, such as laminated iron cores or insulated coils, are unknown. Hence, the material parameters have to be identified by measurements or have to be estimated (Ramesohl *et al.*, 1996). The modelling of microstructures, such as the laminated iron core or resined coils, is memory and computation time expensive, especially if 3D FE models are concerned, as required for the structural-dynamic simulation of complex structures. Here, a material homogenisation technique is applied to cope with this material parameter issue. The mechanical material parameter Young's modulus, Poisson ratio and shear modulus are identified based on numerical and experimental modal analysis (Ewins, 2000). The laminated iron core as well as the resined coils is a transverse isotropic structure. These materials are characterised by symmetry in one plane, for example the x-y plane. Hooke's matrix for transverse isotropic materials with the given plane of symmetry is described by:

Cause	Circumferential ordinal number	Frequency order
1. Stator winding space harmonics	$\nu = p((2mg/N_q^{-1}), \quad g = 0, \pm1, \pm2, \ldots$	p
2. Rotor space harmonics	$\nu = p(2k+1), \quad k = 0, \pm1, \pm2, \ldots$	$(2k+1)p$
3. Rotor reluctance field	$\nu = p(2l+1) + N_1, \quad l = 0, \pm1, \pm2, \ldots$	$(2l+2)p$

Notes: Ordinal numbers and frequencies of important force density waves, where m is the number of phases and N_q denotes the denominator reduced fraction of the slot number per pole and phase

Table I.

	f_1/f_0	ν_1	Field	f_2/f_0	ν_2	Field
A	p	−13	3	p	11	1
B	p	35	3	3p	33	2
C	p	−1	1	p	−1	1

Table II.
Mapping of force density waves to flux density waves

$$H = \begin{pmatrix} \frac{1}{E_x} & -\frac{\nu_{xy}}{E_x} & -\frac{\nu_{xz}}{E_x} & 0 & 0 & 0 \\ -\frac{\nu_{xy}}{E_x} & \frac{1}{E_x} & -\frac{\nu_{xz}}{E_x} & 0 & 0 & 0 \\ -\frac{\nu_{xz}}{E_x} & -\frac{\nu_{xz}}{E_x} & \frac{1}{E_z} & 0 & 0 & 0 \\ 0 & 0 & 0 & \frac{2(1+\nu_{xy})}{E_x} & 0 & 0 \\ 0 & 0 & 0 & 0 & \frac{1}{G_{xz}} & 0 \\ 0 & 0 & 0 & 0 & 0 & \frac{1}{G_{xz}} \end{pmatrix}. \quad (3)$$

In this case, the mechanical material properties can be described by five independent parameters, namely the Young's E_x and E_z in x and z direction, the shear modulus G_{yz} in the y-z plane and the Poisson ration ν_{xy} and ν_{xz} in the x-y and the x-z plane. The homogenised parameters are determined by solving an inverse numerical modal analysis, i.e. optimising these parameters in order to fit the resonant frequencies of the numerical modal analysis to the results of the experimental measurements. To solve this inverse problem a differential evolution algorithm is applied (Price and Storn, 1997). The material parameters, their boundary constraints and relative deviation of the first four resonant frequencies of the laminated iron core as well as the material properties of bulk iron as comparison are collected in Table III. The described method can be applied to determine the mechanical material parameters of transversal isotropic materials in general. However, a drawback is the request of a prototype machine. The resulting material parameters from the discussed approach are used in a next step for the structural-dynamic simulation.

Structural-dynamic simulation

The structural-dynamic simulation is used to determine the deformation of the machine's stator. In the FE model the deformation is represented by the displacements for each node. In the studied case the structural-dynamic simulation is performed by numerical modal analysis, i.e. finding the eigenvalues of the corresponding eigen-problem. Subsequent modal superposition is applied to determine the deformation for each frequency of significant electromagnetic excitation. For this purpose, a 3D model of the complete mechanical structure is built. The frequencies for the modal superposition are selected by amplitude of the force density wave and the eigenvalues of the numerical modal analysis. Since the structural-dynamic simulation is based on a 3D model, the 2D force distribution is transformed from the 2D electromagnetic mesh to the 3D structural-dynamic mesh

Table III. Optimised material parameters and deviation of the first four resonant frequencies

Parameter	*Laminated core*	*Bulk iron*	*Max.*	*Min.*
E_x (GPa)	212.7	210	250	100
E_z (GPa)	26.3	210	100	1
v_{xy}	0.40	0.3	0.6	0.2
v_{xz}	0.14	0.3	0.6	0.01
G_{xy} (GPa)	90.2	80	100	10
Resonant frequencies and relative deviation with material parameter optimization frequencies				
721 Hz	1,947 Hz	1,575 Hz	3,553 Hz	
1.9 per cent	12.3 per cent	0.4 per cent	1.6 per cent	

(Furlan *et al.*, 2003). The setup of the studied motor is shown in Figure 3. The motor has no end-bells, because the shaft is suspended separately. In the studied case, the cooling-fins are modelled with a high level of detail, in order to model the mass and the mass distribution as accurate as possible and to provide a detailed description of the radiating surface. The stator is fixed to a rigid surface. Therefore, the nodes in the structural-dynamic model, which represent this interface, are defined to have no degree of freedom and the displacement is set to zero for all frequencies.

As with the previous example, the frequency $f = 2pf_0$ is chosen to demonstrate the applied approach. The simulated mechanical stress is shown in Figure 4. The vibration mode 2 is dominant for this frequency. This constellation was predicted with the results from the electromagnetic simulation. The cooling fins are oscillating strongly, which

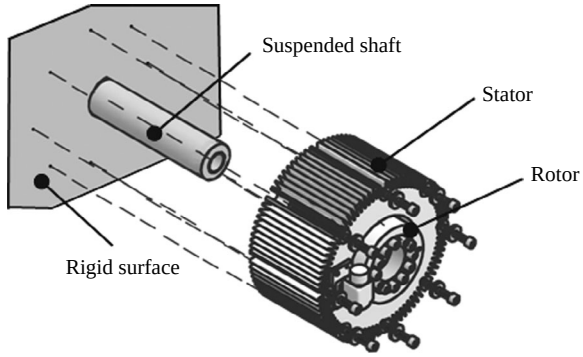

Figure 3.
Structure of motor mounting

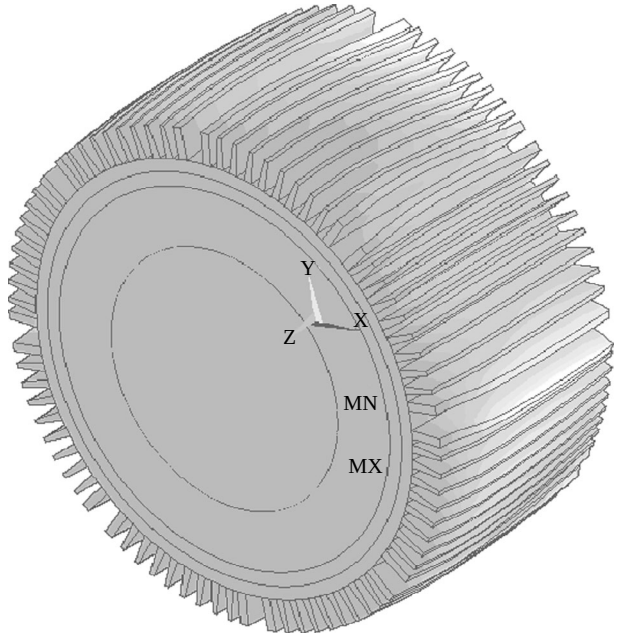

Figure 4.
Deformation of the stator system for the frequency $f = 2pf_0$, the front shows the mounting surface

shows the importance of the detailed model, especially regarding the sound pressure simulation, which will be discussed in the next step.

Acoustic simulation

The radiated sound pressure is calculated in a next step based on the surface velocity v, which is determined from the mechanical deformation d of the surface ($v = j\omega d$). Acoustic noise is the result of the air pressure alternation caused by the oscillation of the motors' surface (Vorländer, 2008). Therefore, only the oscillation of the surface has to be considered and the boundary element method (BEM) acoustic simulation (Furlan *et al.*, 2003). The basic principle is solving the Helmholtz differential equation to determine the sound pressure $\underline{p}$:

$$\Delta\underline{p} + k^2\underline{p} = 0 \tag{4}$$

The wave number k is defined as the fraction of angular frequency ω by the sound velocity c. Since the BEM is applied a new model consisting of the outer surface mesh is built. The mechanical velocity is transformed to this BEM discretisation. The result of this simulation step is the sound pressure and particle velocity on an evaluation surface, in this case a half sphere span around the motor with a distance of 1 m. As a result the sound pressure distribution for the studied excitation with $f = 2pf_0$ and $r = 2$ is shown in Figure 5.The machine shows maxima of the radiated sound pressure in axial direction, whereby the front- and the backside represent minima of the radiation. These characteristics can be explained by the boundary condition of the simulation at the front side and the absence of an end-bell on the backside of the machine.

Results and validation by deformation measurements

The results of the simulation discussed so far are the force distribution acting on the stator teeth, the deformation of the stator and the radiated sound pressure surrounding the machine. For the structural-dynamic simulation the fitted material parameters for the homogenisated model are used. Deformation measurements are performed to validate

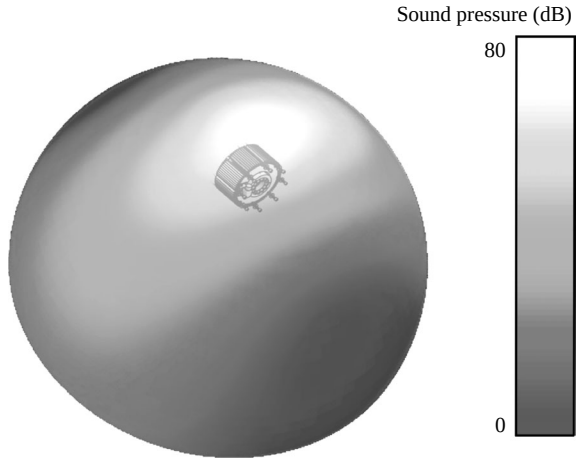

Figure 5.
Sound pressure indicated in dB referred to undisclosed reference

the multiphysics simulation chain. The acceleration is measured on the surface of the electrical machine at 16 different positions (Genta, 1999). Figure 6 shows the set-up of the practical experiment. The acceleration is measured employing a dual channel signal analyser. One of the two accelerometers is kept at a constant position. The second sensor is placed at various measurement points on the surface of the machine. By double integration of the acceleration a, the displacement d at the points can be calculated ($d = -(1/\omega^2)a$).

The data for the displacement on the surface of the 3D FE model are evaluated at the measured positions. The deformation shape and the magnitudes for the first eight mode numbers are compared. As an example, the deformation at the studied excitation at frequency $f = 2pf_0$ is shown in Figure 7. The left diagram illustrates the mode shapes; the right diagram compares the amplitudes of the deformation according to its modal number. The amplitude of dominant deformation with the modal number 2 differs less than 10 per cent from the measurements and simulation. As expected, form the force excitation the mode number of the deformation is $r = 2$. The measurements reveal comparable high amplitude with the mode number one. The reason for this may be found in the eccentricity, for example caused by an eccentric rotor adjustment, or a magnetic anisotropy. Since the frequency of the deformation with mode number one is $f = 2pf_0$ the eccentricity is static. Indications for a static eccentricity are also found in other frequency components of the measurements. Since rotor and stator are mounted individually onto the application, static eccentricity seams unavoidable.

Conclusions

In this paper, the electromagnetic excited structure-borne sound and air-borne noise of an AC servo drive is analysed. An automated multiphysics simulation model applying weak numerical coupling is presented and the important aspects for audible noise simulations of electrical machines are pointed out. In particular, the analysis of the electromagnetic forces is discussed. With these results an acoustic optimisation of the motor can be performed. This will be the topic of further work from the authors at

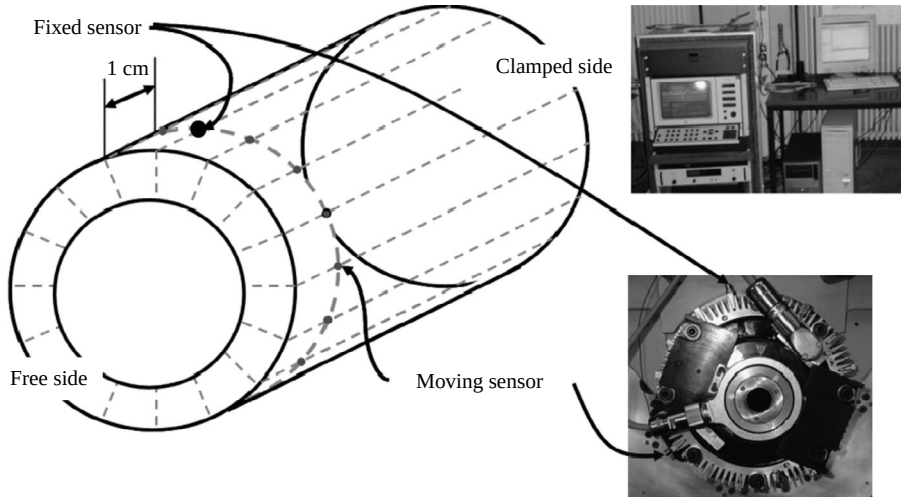

Figure 6.
Experimental set-up for the acceleration measurements

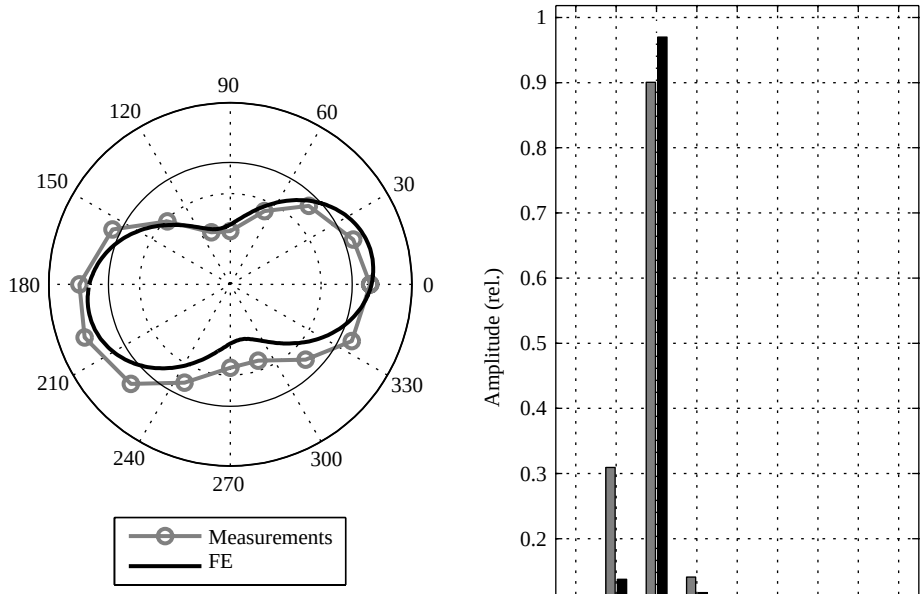

Figure 7.
Comparison of simulation and measurement

Note: Displacement on the surface of the stator with $f = 2pf_0$

Institute of Electrical Machines (IEM). In contrast to commonly used mechanical material parameters a material homogenisation is performed for the structural-dynamic simulation. It is shown, that this kind of material parameters yields a very accurate structural dynamic model. The presented approach for the material homogenisation is of general application. However, it is dependent on the availability of a prototype and required measurement data from it. A generalisation of this approach is planned for future studies. It can be stated that the results of this simulation with the optimised material parameters are in good agreement with the measurements performed.

The simulation model reveals a realistic pattern of the structure-borne sound and acoustic radiation. Therefore, it is possible to benchmark the acoustic behaviour of optimized designs before building a prototype.

References

Ewins, D. (2000), *Modal Analysis*, Research Studies Press Ltd, Baldock.

Furlan, M., Cernigoj, A. and Boltezar, M. (2003), "A coupled electromagnetic-mechanical-acoustic model of a DC electric motor", *COMPEL: International Journal for Computation and Mathematics in Electrical and Electronic Engineering*, Vol. 22 No. 4, pp. 1155-65.

Garvey, S. (1989), "The vibrational behaviour of laminated components in electrical machines", *Fourth International Conference on Electrical Machines and Drives*, pp. 226-31.

Genta, G. (1999), *Vibartions of Structures and Machines – Practical Aspects*, Springer, Berlin.

Gieras, J., Wang, C. and Lai, J.C. (2006), *Noise of Polyphase Electric Motors*, CRC Press, Boca Raton, FL.

Herranz Gracia, M. (2008), *Methoden zum Entwurf von robusten Stellantrieben unter Berücksichtigung fertigungsbedingter Abweichungen*, Shaker, Aachen.

Jordan, H. (1950), *Geräuscharme Elektromotoren*, W. Girardet, Essen.

Price, K. and Storn, R. (1997), "Differential evolution: numerical optimization made easy", *Dr. Dobb's Journal*, April, pp. 18-24.

Ramesohl, I., Henneberger, G., Kuppers, S. and Hadrys, W. (1996), "Three dimensional calculation of magnetic forces and displacements of a claw-pole generator", *IEEE Transactions on Magnetics*, Vol. 32 No. 3, pp. 1685-8.

van der Giet, M., Rothe, R. and Hameyer, K. (2009), "Asymptotic Fourier decomposition of tooth forces in terms of convolved air gap field harmonics for noise diagnosis of electrical machines", *COMPEL: International Journal for Computation and Mathematics in Electrical and Electronic Engineering*, Vol. 28 No. 4, pp. 804-18.

Vorländer, M. (2008), *Auralization – Fundamentals of Acoustics, Modelling, Simulation, Algorithms and Acoustic Virtual Reality*, Springer, Berlin.

About the authors

David Franck received his Diploma in Electrical Engineering in 2008 as Engineer from the Faculty of Electrical Engineering and Information Technology at RWTH Aachen University. Since, 2008 he has worked as a researcher at IEM at RWTH Aachen University. He is currently working towards his doctoral degree in the area of noise and vibration of electrical machines. David Franck is the corresponding author and can be contacted at: david.franck@iem.rwth-aachen.de

Michael van der Giet received his Diploma in Electrical Engineering in 2004 as Engineer from the Faculty of Electrical Engineering and Information Technology at the RWTH Aachen University, Aachen, Germany. Since 2004, he has worked as a researcher at the Institute of Electrical Machines at the RWTH Aachen University. He is currently working towards his doctoral degree in the area of noise and vibration of electrical machines.

Kay Hameyer (M'96-SM'99) received the MSc degree in Electrical Engineering from the University of Hannover, Hannover, Germany, and the PhD degree from the University of Technology Berlin, Berlin, Germany. After his university studies, he was with Robert Bosch GmbH, Stuttgart, Germany, as a Design Engineer for permanent-magnet servo motors and electrical energy-supply system components. In 1988, he became a Member of the Staff of the University of Technology Berlin. He was a Full Professor of numerical field computations and electrical machines with the Katholieke Universiteit Leuven, Belgium, until February 2004. In 2005, he was with Poznan University of Technology, Poznan, Poland. He is currently a Full Professor, the Director of the Institute of Electrical Machines, and the holder of the Chair Electromagnetic Energy Conversion at RWTH Aachen University, Aachen, Germany, where he has been the Dean of the Faculty of Electrical Engineering and Information Technology from 2007 to 2009. His research interests include numerical field computation and simulation, design of electrical machines, particularly permanent-magnet excited machines and induction machines, and numerical optimization strategies.